FULL PAPER

The study of range-scaling transformation of nanoparticle compounds on thin films of gold-centered monolayer protected nanoparticles by molecular modeling

Mehrdad Shahpar[a],*, Sharmin Esmaeilpoor[b]
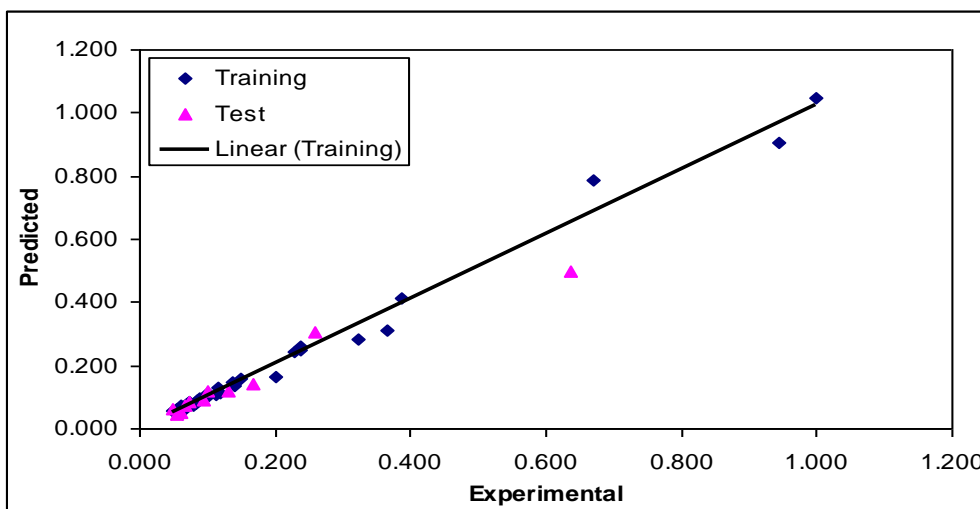
[a]Director of Ilam Petrochemical Company.

[b]Department of Chemistry, Payame Noor University, P.O. BOX 19395-4697, Tehran,Iran.

ABSTRACT: A quantitative structure–retention relation (QSRR) study was conducted on the range-scaling transformation (Xa) of the nanoparticle compounds which obtained by comprehensive two-dimensional gas chromatography (GC×GC) stationary phases consisting of thin films of the gold-centered monolayer protected nanoparticles (MPNs) system. The genetic algorithm was used as descriptor selection and model development method. Modeling of the relationship between the selected molecular descriptors and the retention time was achieved by linear (partial least square; PLS) and nonlinear (Levenberg-Marquardt artificial neural network; L-M ANN) methods. Linear and nonlinear methods resulted in an accurate prediction whereas more accurate results were obtained by L-M ANN model.

KEYWORDS: Nanoparticle compounds; Gold-centered monolayer protected nanoparticles; Comprehensive two-dimensional gas chromatography; QSRR; Levenberg-Marquardt artificial neural network.

GRAPPHICAL ABSTACT:

Introduction

For decades, chromatographers have utilized nanometersized materials in the development of highly efficient chromatographic stationary phases. These materials offer a variety of advantages from improved mass transfer characteristics to greater stability of traditional polymer phases by incorporating nanoparticle additives. Nanoparticles on the order of 10 nm in diameter have also been used to stabilize polymer stationary phases for gas

*Corresponding author: Radwa T. Rashad, Email: radwa_rashad267@yahoo.com, Tel: +201060750024, Fax: 0502247800

chromatography (GC), similar in concept to that for support coated open tubular columns. The unaccompanied use of nanoparticles as chromatographic stationary phases has been put forth. Both silica and polymer nanoparticles have been applied in electrophoretic chromatography as a stationary phase [1-4]. In separation science, nanoparticles have been used as novel stationary phases to provide high separation efficienc for various analytes. Since the nanoparticles are too small to be packed into the column, they were used mostly as pseudostationary phases to enhance the separation performance [5–8]. The most improtant advantage of the GC×GC over conventional GC is its increased resolution power as the peak capacity in GC×GC is the product of the peak capacity of each separation column [9, 10]. The use of monolayer-protected gold nanoparticles (MPNs) as a stationary phase for open tubular GC has been reported [11-13]. The electronic interactions of the polar stationary phase material with itself and/or the capillary wall tend to cause non-uniform deposition within the capillary. After initial failures for satisfactory polar MPN column (4-chlorobenzenethiol MPNs) production using the procedure established for the nonpolar MPN column (dodecanethiol MPN column) production, it was determined that a "slightly polar" capillary would be used instead of the deactivated silica that is usually purchased for column preparation. This transformation was applied to the retention time data of 55 probe analytes of varying chemical make-up. To calculate Xa, one first makes a list of the relative retention times for all the analytes in the study, with the relative retention time equal to the retention time minus the dead time [14, 15]. The Xa for a given analyte is calculated by dividing the relative retention time of the analyte to the relative retention time of the longest retained analyte. This normalization approach allows for an objective comparison between two stationary phases. In this instance the longest retained analyte was 1-hexanol for 4-chlorobenzenethiol MPNs stationary phase column. In addition, the chromatographic retention prediction methodologies can be valuable starting points for developing the GC method. A promising approach is the use of quantitative structure–retention relationship (QSRR) [17-19]. In chromatography, QSRR have been applied to: (i) gain a better understanding of the molecular mechanism of the chromatographic separation process; (ii) identify the most informative structure related properties of analytes; (iii) characterize stationary phases, and (iv) predict retention for new analytes [17]. There is a trend to develop QSRR using a variety of methods. In particular, genetic algorithm (GA) is frequently used as search algorithms for variable selection in chemometrics and QSRR. The GA provides a "population" of models, from which it could be difficult to identify the most significant or relevant models (which may be preferred in certain uses such as, regulatory toxicology prediction) [20]. Partial least square (PLS) is the most commonly used multivariate calibration method. Moreover, non-linear statistical treatment of QSRR data is expected to provide models with better predictive quality compared with the related PLS models. In this perspective, artificial neural network (ANN) modelling has become quite common in the QSRR field [21-23]. Extensive use of ANN, which does not require the "a priori" knowledge of the mathematical form of the relationship between the variables, largely rests on its flexibility functions of any complexity can be apply. In this research, GA-PLS and L-M ANN were employed to generate the QSRR models that correlate the structure of the nanoparticles.

2 - Material and methods

2.1 - Data set

Range-scaling transformation (Xa) of 55 nanoparticle compounds are presented in Table 1 [24]. Sample components are separated, identified, and measured by the 4-chlorobenzenethiol MPNs stationary phase include complementary separations such as two-dimensional GC and potential utilization within a model system for a micro-fabricated GC (GC). The efficiency and speed achieved with the dodecanethiol MPN stationary phase in the 100 m i.d. capillary with a short column length (1.5 m) dictates that it be used as the first column. All the chromatograms were obtained with an injection source and FID temperature of 250 0C. The inlet pressure was maintained at 48,000 Pa with a variable split as stated, while the auxiliary pressure (column pressure) was varied independently as dictated by the experimental method being employed. The oven temperature was constant at 50 ◦C unless otherwise noted. For the GC experiments, either a or 15m poly (ethyleneglycol) or 4-chlorobenzenethiol MPNs column with a 250 m i.d. and 0.2 m film thickness (IMMOWax, Agilent Technologies, Palo Alto, CA, USA) was used as the first column of the GC $\times$ GC system, and a dodecanethiol MPN column as the second column.

2.2 - **Molecular modeling and theoretical** molecular descriptors

The derivation of theoretical molecular descriptors proceeds from the chemical structure of the compounds. To calculate the theoretical descriptors, molecular structures were constructed with the aid of HyperChem version 7.0. The final geometries were obtained with the semi-empirical AM1 method using the HyperChem program. The molecular structures were optimized using Fletcher- Reeves algorithm until the root mean square gradient was 0.01 kcal mol-1. Some quantum descriptor such as orbital energy of HOMO was calculated using the HyperChem software. The resulted

geometry was transferred into Dragon program, to calculate 1497 descriptors, which was developed by Todeschini et al [25]. To reduce the original pool of the descriptors to an appropriate size, the objective descriptor reduction was performed using various criteria. Reducing the pool of descriptors eliminates those descriptors which contribute either no information or whose information content is redundant with other descriptors present in the pool.

2.3 - **Computer hardware and software**

All calculations were run on a HP Laptop computer with AMD Turion64X2 processor with windows XP operating system. The optimizations of molecular structures were done by the HyperChem 7.0 (AM1 method) and descriptors were calculated using the Dragon Version 3.0 software's. MINITAB software version 14 was used for the simple PLS analysis. Cross validation, GA-PLS, GA-KPLS and other calculation were performed in the MATLAB (Version 7, Mathworks, Inc.) environment.

2.4 - **Nonlinear model**
2.5 - **Artificial neural network**

An artificial neural network (ANN) with a layered structure is a mathematical system that stimulates biological neural network, consisting of computing units named neurons and connections between neurons named synapses [25-29]. All the feed-forward ANN used in this study are three-layer networks. Each neuron in any layer is fully connected with the neurons of a succeeding layer. Fig. 1 shows an example of the architecture of such ANN. The Levenberg–Marquardt back propagation algorithm was used for ANN training and the linear functions were used as the transformation functions in hidden and output layers.
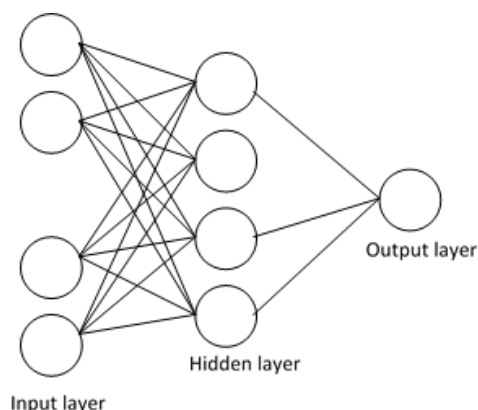
FIG. 1. *Used three layer ANN*

3.1 - Results of the L-M ANN model

With the aim of improving the predictive performance of the nonlinear QSRR model, L-M ANN modeling was performed. The networks were generated using the seven descriptors appearing in the GA-PLS models as their inputs and Xa as their output. A three-layer network with a sigmoid transfer function was designed for each ANN. Before training the networks, the input and output values were normalized between -1 and 1. The network was then trained using the training set by the back propagation strategy for optimization of the weights and bias values. The procedure for optimization of the required parameters is given elsewhere [30]. The proper number of nodes in the hidden layer was determined by training the network with different number of nodes in the hidden layer. The root-mean-square error

(RMSE) value measures how good the outputs are in comparison with the target values. It should be noted that, for evaluating the overfitting, the training of the network for the prediction of Xa must stop when the RMSE of the prediction set begins to increase while RMSE of calibration set continues to decrease [31]. Therefore, training of the network was stopped when overtraining began. All of the above mentioned steps were carried out using basic back propagation, conjugate gradient and Levenberge-Marquardt weight update functions. It was realized that the RMSE for the training and test sets are minimum when four neurons were selected in the hidden layer and the learning rate and the momentum values were 0.8 and 0.4, respectively. Finally, the number of iterations was optimized with the optimum values for the variables. It was realized that after 18 iterations, the RMSE for prediction set were minimum. The R^2 and RE for training and test sets were (0.964, 0.911) and (8.70, 13.20), respectively. The values of experimental, calculated, RE and RMSE are shown in Table 1.

Inspection of the results reveals a higher R^2 and lowers other values parameter for the test set compared with their counterparts for other models. Plots of predicted Xa versus experimental Xa values by L-M ANN for training and test sets are shown in Fig. 2.
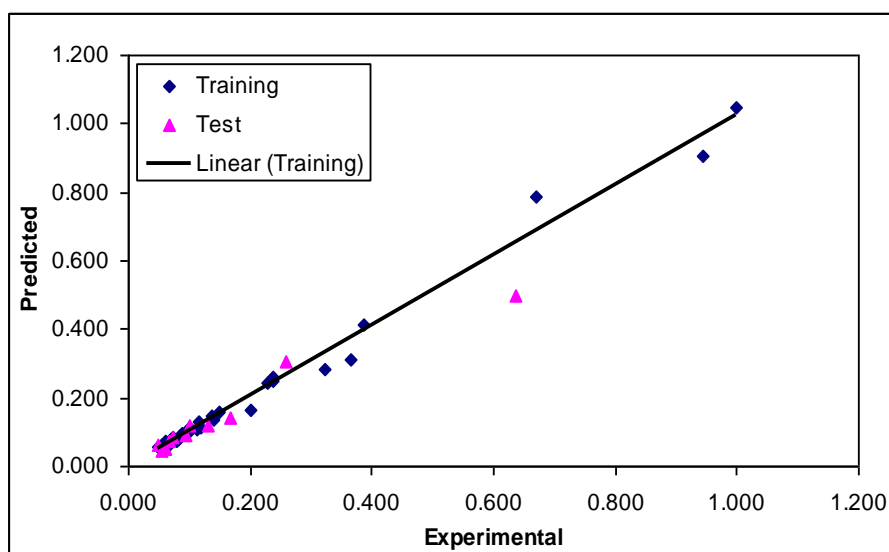
Fig.2. *Plot of predicted Xa obtained by L-M ANN against the experimental values.*

Table 1*. The data set and the corresponding observed and predicted Xa values by L-M ANN for the training and test set.*

No	Name	Xa Exp	Xa Cal	RE	RMSE
Training set					
1	Hexane	0.050	0.054	8.000	0.004
2	Cyclopentane	0.051	0.058	13.726	0.007
3	1,1,1-Trichloroethane	0.052	0.057	9.615	0.005
4	Triethylamine	0.053	0.049	7.547	0.004
5	Hexyne	0.054	0.052	3.704	0.002
6	Acetonitrile	0.055	0.065	18.182	0.010
7	Ethyl acetate	0.056	0.059	5.357	0.003
8	Heptene	0.058	0.063	8.621	0.005
9	Tetrahydrofuran	0.059	0.049	16.949	0.010
10	1,2-Dichloroethane	0.060	0.059	1.667	0.001
11	Proprionitrile	0.062	0.071	14.516	0.009
12	Toluene	0.063	0.068	7.937	0.005
13	2-Butanol	0.064	0.060	6.250	0.004
14	Ethyl formate	0.067	0.061	8.955	0.006
15	Benzene	0.068	0.066	2.941	0.002
16	trans-1,2 Dimethylcyclohexane	0.070	0.079	12.857	0.009
17	Heptane	0.071	0.077	8.451	0.006
18	Trichloromethane (chloroform)	0.072	0.075	4.167	0.003
19	n-Butylamine	0.073	0.085	16.438	0.012
20	Cyclooctane	0.080	0.076	5.000	0.004
21	Butyl formate	0.081	0.078	3.704	0.003
22	1-Bromopentane	0.083	0.082	1.205	0.001
23	2-Pentanone	0.084	0.093	10.714	0.009
24	1-Nonene	0.088	0.096	9.091	0.008
25	Butyl acetate	0.096	0.094	2.083	0.002
26	Ethylbenzene	0.099	0.106	7.071	0.007

27	1-Chlorohexane	0.101	0.114	12.871	0.013
28	Pyridine	0.102	0.108	5.882	0.006
29	Chlorobenzene	0.112	0.106	5.357	0.006
30	2-Pentanol	0.116	0.131	12.931	0.015
31	2-Hexanone	0.118	0.115	2.542	0.003
32	1-Nonyne	0.137	0.149	8.759	0.012
33	1-Butanol	0.141	0.137	2.837	0.004
34	Decane	0.148	0.159	7.432	0.011
35	1,3,5-Trimethyl benzene (mesitylene)	0.201	0.162	19.403	0.039
36	Methyl phenyl ether(anisole)	0.229	0.246	7.424	0.017
37	Bromobenzene	0.237	0.251	5.907	0.014
38	1-Nitrobutane	0.239	0.261	9.205	0.022
39	2-Heptanone	0.322	0.285	11.491	0.037
40	1-Pentanol	0.365	0.311	14.795	0.054
41	1-Bromoheptane	0.388	0.416	7.217	0.028
42	Octanal	0.670	0.785	17.164	0.115
43	Cyclohexanol	0.944	0.907	3.920	0.037
44	1-Hexanol	1.000	1.048	4.800	0.048
Test set					
45	Cyclohexane	0.050	0.060	20.000	0.010
46	Cycloheptane	0.056	0.047	16.071	0.009
47	1-Heptyne	0.060	0.053	11.667	0.007
48	1-Chlorobutane	0.067	0.071	5.970	0.004
49	Nitroethane	0.074	0.083	12.162	0.009
50	1,1,2-Trichloroethane	0.093	0.091	2.151	0.002
51	p-Xylene	0.101	0.117	15.842	0.016
52	Hexanal	0.131	0.121	7.634	0.010
53	Bromohexane	0.168	0.144	14.286	0.024
54	Heptanal	0.259	0.304	17.375	0.045
55	Cyclohexylamine	0.638	0.497	22.100	0.141

which would be compared with the values of 13.20 and 0.911, respectively, for the L-M ANN model. Comparison between these values and other statistical parameters reveals the superiority of the L-M ANN model over other model. The statistical parameters reveal the high predictive ability of the L-M ANN model. The whole of these data clearly displays a significant improvement in the QSRR model consequent to nonlinear statistical treatment. Obviously, there is a close agreement between the experimental and predicted Xa and the data represent a very low scattering around a straight line with respective slope and intercept close to one and zero. As can be seen in this section, the L-M ANN is more reproducible than GA-PLS for modeling the GC×GC range-scaling transformation of nanoparticle compounds.

3.2 - Model validation and statistical parameters

The applied internal (leave-group-out cross validation (LGO-CV)) and external (test set) validation methods were used for the predictive power of models. In the leave-

group-out procedure one compound was removed from the data set, the model was trained with the remaining compounds and used to predict the discarded compound. The process was repeated for each compound in the data set. The predictive power of the models developed on the selected training set is estimated on the predicted values of test set chemicals. The data set should be divided into three new sub-data sets, one for training (calibration and prediction), and the other one for testing. The calibration set was used for model generation. The prediction set was applied deal with overfitting of the network, whereas test set which its molecules have no role in model building was used for the evaluation of the predictive ability of the models for external set.

On the other hand, by means of training set, the best model is found and then, the prediction power of it is checked by test set, as an external data set. In this work, 80% of the database was used for training set and 20% for test set, randomly (in each running program, from all 55 components, 44 components are in training set and 11 components are in test set).

The result clearly displays a significant improvement in the QSRR model consequent to non-linear statistical treatment and a substantial independence of model prediction from the structure of the test molecule. In the above analysis, the descriptive power of a given model was measured to predict the partition of the unknown nanoparticle compounds. For the constructed models, some general statistical parameters were selected to evaluate the predictive ability of the models for Xa values. In this case, the predicted Xa of each sample in prediction step was compared with the experimental acidity constant. Root mean square error (RMSE) is a measurement of the average difference between predicted and experimental values, at the prediction step. RMSE can be interpreted as the average prediction error, expressed in the same units

as the original response values. Its small value indicates that the model predicts better than chance and can be considered statistically significant. The RMSE was obtained by the following formula:

$$(1)\quad RMSE = [\frac{1}{n}\sum_{i=1}^{n}(y_i - y_i^{\wedge})^2]^{\frac{1}{2}}$$

The other statistical parameter was relative error (RE), showing the predictive ability of each component, and is calculated as:

$$(2)\quad RE(\%) = 100 \times \left[\frac{1}{n}\sum_{i=1}^{n}\frac{(y_i^{\wedge} - y_i)}{y_i}\right]$$

The predictive ability was evaluated by the square of the correlation coefficient (R^2) which is based on the prediction error sum of squares and was calculated by following equation:

$$(3)\quad R^2 = \frac{\sum_{i=1}^{n}(y_i^{\wedge} - \bar{y})}{\sum_{i=1}^{n}(y_i - \bar{y})}$$

Where y_i is the experimental Xa in the sample i, $\hat{y}_i$ represented the predicted Xa in the sample i, $\bar{y}$ is the mean of experimental Xa in the prediction set and n is the total number of samples used in the test set. The main aim of the present work was to assess the performances of the GA-PLS and L-M ANN for modeling the Xa of nanoparticle compounds. The procedures of modeling including descriptor generation, splitting of the data, variable selection and validation were the same as those performed for modeling of the range-scaling transformation of nanoparticle compounds.

Interpretation of descriptors

In GC×GC, the entire sample is submitted to two online GC separations involving different properties of analytes, i.e., the volatility related to the carbon atom number and the polarity related to the chemical group. In the chromatographic retention of

compounds in the polar stationary phases is related to the induced forces that are very important in retention of the compounds. The induced forces are related to the dipolar moment, which should stimulate dipole-induced dipole or Debye forces interactions. Also, it is related to the dispersion forces. The dispersion forces related to steric factors, molecular size and branching. Constitutional descriptors are the most simple and commonly used descriptors, reflecting the molecular composition of a compound without any information about its molecular geometry. The most common constitutional descriptors are the number of atoms, number of bound, absolute and relative numbers of the specific atom type, absolute and relative numbers of the single and etc. The hydrogen bonding was related to the number of Hydrogen atoms (nH). Hydrogen-bonding may be divided into an electrostatic term and a polarization/charge transfer term. A particularly strong type of polar interaction occurs in molecules where a hydrogen atom is attached to an extremely electron-hungry atom such as oxygen, nitrogen, or fluorine. Understandably, hydrogen bonding plays a significant role in retention behavior.

The geometrical descriptors are suitable for complex-behaved properties, because they take into account the 3D-arrangement of the atoms without ambiguities and also because they do not depend on the molecular size. This feature makes it probable that the geometrical descriptors appear in the resulting model. The SPAN is a size descriptor definite as the radius of the smallest sphere, centered on the centre of mass, completely enclosing all atoms of a molecule. 3D-MoRSE (3D-MOlecule Representation of Structures based on Electron diffraction) descriptors are based on the idea of obtaining information from the 3D atomic coordinates by the transform used in electron diffraction studies. These descriptors are calculated by summing atom

weights viewed by a divergent angular scattering function. Although functional group, atom center fragment, constitutional and geometrical descriptors are often successful in rationalizing partition of nanoparticle on columns, they cannot account for conformational changes and they do not provide information about electronic influence through bonds or across space. For that reason, quantum chemical descriptors are used in developing QSRR.

Charge descriptors were defined in terms of atomic charges and used to describe the electronic aspects for both of the whole molecule and particular regions such as, atoms, bonds, and molecular fragments. Electrical charges in the molecule are the driving force of electrostatic interactions, and it is well known that local electron densities or charge play a fundamental role in many physic-chemical properties and receptors-ligand binding affinity. Thus, charge based descriptors have been widely employed as chemical reactivity indices or as measures of weak intermolecular interactions. Many quantum chemical descriptors are derived from the partial charge distribution in a molecule or from the electron densities on particular atoms. Relative positive charge (RPCG) is the quotient between maximum atomic positive charge in the molecule and positive atomic charge in the molecule. It contains electronic information to describe the molecule, and therefore it encodes features responsible for interaction between molecules and the modified reversed stationary phase.

Quantum chemical descriptors can give great insight into structure and reactivity and can be used to establish and compare the conformational stability, chemical reactivity, and inter-molecular interactions. They include thermodynamic properties (system energies) and electronic properties (HOMO energy). Quantum chemical descriptors were defined in terms of atomic charges and used to describe electronic

aspects both of the whole molecule and of particular regions, such atoms, bonds, and molecular fragments. Electronic properties may play a role in the magnitude in a biological activity, along with structural features encoded in indexes. HOMO as an electron donor represents the ability to donate an electron. The HOMO energy plays a very important role in the nucleophylic behavior and it represents molecular reactivity as a nucleophyle. Good nucleophyles are those where the electron residue is high lying orbital [31].The particle size, hydrogen bonding, and electrostatic interactions are the likely three factors controlling the Xa of the nanoparticles. All the descriptors involved in the model may account for the structure responsible for the Xa of these compounds.

Conclusion

In this research, an accurate QSRR model for estimating the range-scaling transformation (Xa) of nanoparticle compounds was developed by employing the GA-PLS and L-M ANN techniques. These models have good predictive capacity and excellent statistical parameters. A comparison between these models revealed the superiority of the L-M ANN to GA-PLS model. It is easy to notice that there was a good prospect for the L-M ANN application in the QSRR modeling. It can also be used successfully to estimate the Xa for new compounds or for other compounds whose experimental values are unknown. This indicates that Xa of nanoparticle compounds possesses some nonlinear characteristics.

References

1.   Brown DB, Wilson MR, MacNee M (**2001**) *Appl. Pharmacol* 175: 191-199.

2.   Inoue K, Takano H, Yanagisawa R, Sakurai M, Ichinose T, Sadakane K, Yoshikawa T (**2001**) *Respir. Res* 6:106-111.

3. Buzorius G, Zelenyuk A, Brechtel F, Imre D (**2002**) *Geophys Res Let* 29:1974–1978.

4. Chong-Shu Zhu, Cheng-Chieh Chen, Jun-Ji Cao, Chuen-Jinn Tsai, Ch.C.-K. Chou, Shaw-Chen Liu, Gwo-Dong Roam (**2010**) *Atmos. Environ* 44: 2668-2673.

5.   Hang Ho Si, Zhen Yu J (**2004**) *J. Chromatogr*. A1059: 121–129.

6. Dallüge J, Rijn M, Beens J, Vreuls RJJ, Brinkman UA (**2002**) J. *Chromatogr. A* 965:207-214.

7.   Adam F, Bertoncini F, Brodusch N, Durand E, Thiebaut D, Espinat D, Hennion MC (**2007**) *J. Chromatogr. A* 1148: 55–64.

8.   Hyölyläinen T, Kallio M, Shimmo M, Saamio K, Hartonen K, Riekkola ML (**2003**) Presentation at the First International Symposium on Two-Dimensional Gas Chromatography, Volendam, The Netherlands.

9. Muhlen C, Alcaraz Zini C, Bastos Caramao E, Marriott Ph (**2008**) *J. Chromatogr*. A1200: 34–42.

10. Hamilton JF, Webb PJ, Lewis AC, Hopkins JR, Smith S, Davy P (**2004**) *Atmos. Chem. Phys* 4: 1279-1290.

11.   Ochiai N, Ieda T, Sasamoto K, Fushimi A, Hasegawa Sh, Tanabe K, Kobayashi Sh (**2007**) *J. Chromatogr. A* 1150: 13–20.

12. Leban J, Baierl M, Mies J, Trentinaglia V, Rath S, Kronthaler K, Wolf K (**2007**) *Chem. Lett* 17:5858–5862.

13.   Gajewicz A, Haranczyk M, Puzyn T (**2010**) *Atmos. Environ* 44: 1428-1436

14.   Niazi A, Jameh-Bozorghi S, Nori-Shargh D (**2008**) *J. Hazard. Mater*. 151: 603-609

15.   Noorizadeh H, Esmaeilpoor Sh, Moghadam Z, Nosratolahy Sh (**2014**) *ICC* 4: 283-299

16. Woo SH, Jeon ChO, Yun YS, Choi H, Lee ChS, Lee DS (**2009**) *J. Hazard. Mater* 161: 538–544

17.   Krämer N, Boulesteix AL, Tutz G (**2008**) *Chemom. Intell. Lab. Syst* 94: 60–69.

18. Todeschini R, Consonni V, Mauri A, Pavan M (**2003**) DRAGON-Software for the calculation of molecular descriptors. Version 3.0 for Windows.

19.   Goldberg DE (**2000**) Genetic Algorithms in Search, Optimization and Machine Learning, Addison-Wesley–Longman, Reading, MA, USA.

20. Esmaeilpoor Sh, Shirzadi Z, Noorizadeh H (2014) *ICC* 2: 56-71.

21. Sousa JAD, Hemmer MC, Casteiger J (**2002**) *Anal. Chem.* 74, 80-88.

22. Depczynski U, Frost VJ, Molt K (**2000**) factors in principal component regression. *Anal. Chim. Acta* 420: 217-227.

23. Wold S, Sjostrom M, Eriksson L (**2001**) *Lab. Syst* 58: 109-114.

24.   Shahpar M, Esmaeilpoor Sh (**2017**) Asian *J. Green Chem* 2: 116-129

25.   Rosipal R, Trejo LJ (**2001**) *J. Mach. Learning Res* 2: 97-110.

26. Kim K, Lee JM, Lee IB (**2005**) *Chemom. Intell. Lab. Syst* 79: 22-30.

27.   Acevedo-Martınez J, Escalona-Arranz JC, Villar-Rojas A, Tellez-Palmero F, Perez-Roses R, Gonzalez L, Carrasco-Velar R (**2006**) *J. Chromatogr. A* 1102: 238-244.

28. Shahpar M, Esmaeilpoor Sh, Advanced QSRR *Chem. Method.* Articles in Press

29. Golbraikh A, Tropsha A (**2002**) Beware of q2. J. Mol. Graphics Modell 20: 269-276.

30. Todeschini R, Consonni V (**2000**) Handbook of Molecular Descriptors, *Wiley-VCH, Weinheim, German.*

How to cite this manuscript: Mehrdad Shahpara*, Sharmin Esmaeilpoorb. The study of range-scaling transformation of nanoparticle compounds on thin films of gold-centered monolayer protected nanoparticles by molecular modeling. Asian Journal of Nanoscience and Materials, 2018, 1, 1-10.